Environmental Research 288 (2026) 123286

Contents lists available at ScienceDirect

Environmental Research

journal homepage: www.elsevier.com/locate/envres

Climate change reflected in 40-year isotopic composition trends of precipitation in Slovenia

Jan Gačnik [a,*], Klara Žagar [a], István Gábor Hatvani [b,c], Zoltán Kern [b,c], Polona Vreča [a]

[a] Department of Environmental Sciences, Jožef Stefan Institute, Jamova cesta 39, 1000, Ljubljana, Slovenia
[b] Institute for Geological and Geochemical Research, HUN-REN Research Centre for Astronomy and Earth Sciences, Budaörsi út 45, H-1112, Budapest, Hungary
[c] HUN-REN CSFK, MTA Centre of Excellence, Konkoly Thege Miklós út 15-17, H-1121, Budapest, Hungary

ARTICLE INFO

Keywords:
Precipitation stable isotopes
Trend analysis
Hilbert-Huang transform
Ensemble empirical mode decomposition
HYSPLIT

ABSTRACT

Long-term monitoring of stable isotopes in precipitation ($\delta^{18}O$, δ^2H), alongside meteorological data, is key to understanding how large-scale hydroclimate variability influences regional and local climate. This study presents one of the longest records in Central and Southeastern Europe: the multi-decadal (1981–2024) dataset of monthly composite precipitation stable isotope records from Ljubljana, Slovenia. The $\delta^{18}O$, δ^2H, and *d*-excess values are increasing (+0.02 ‰, +0.18 ‰, and +0.05 ‰ per year, respectively), consistent with regional warming. Seasonal patterns were evident, with elevated *d*-excess values during autumn. The decomposition of the $\delta^{18}O$, δ^2H and *d*-excess time series using Hilbert-Huang Transform revealed statistically significant annual oscillations in all variables. These oscillations correlated strongly with the annual oscillation of temperature, but a lag of 2–3 months was identified for *d*-excess. Lower-frequency (multi-year) oscillations of *d*-excess were also observed. HYSPLIT back-trajectory analysis confirmed a significant contribution of Mediterranean-sourced air masses to autumn precipitation, but did not explain *d*-excess oscillations. Similar results were observed also for coastal (Portorož, Slovenia) and continental (Vienna, Austria) stations. The findings imply an accelerating, exponential-like isotopic response to warming that has already propagated into the water cycle, providing isotope evidence that precipitation-surface water-groundwater interactions in investigated region changed in last decade.

1. Introduction

Stable isotope ratios ($^{18}O/^{16}O$, $^2H/^1H$, expressed in standard δ notation as $\delta^{18}O$ and δ^2H) of precipitation collected at monitoring stations worldwide are well-known sensitive indicators of hydroclimatic variations (Dee et al., 2023). Depending on the precipitation collection frequency (e.g., events, monthly composites) and timeframe (years, decades) precipitation stable isotope records can be used to study large-scale atmospheric circulations (Baldini et al., 2008; Birks and Edwards, 2009; Brenčič et al., 2015; Liu et al., 2010; Welker, 2012); however, isotope time series of long temporal coverage are needed to detect multi-decadal climatic oscillations (Klaus et al., 2015; Lykoudis and Argiriou, 2011; Vystavna et al., 2020). Isotopic composition of precipitation depends on various conditions and meteorological parameters which are related to the atmospheric circulation patterns and their spatiotemporal distribution (Dansgaard, 1964; Puntsag et al., 2016; Rozanski et al., 1993). It is known that the source of water vapor and air flow direction influences the isotopic composition of precipitation (Bailey et al., 2019; Natali et al., 2023). However, little is known about the dependence between global and regional atmospheric circulation patterns responsible for precipitation generation and the stable isotopic composition of the resulting precipitation (Brenčič et al., 2015; Comas-Bru et al., 2016).

Coordinated long-term monitoring of stable isotopes in precipitation, coupled with basic meteorological parameters such as air temperature and precipitation amount, are essential to (i) better understand the impact of larger scale hydroclimate variation on regional and local climate variability, and (ii) to help interpret long-term hydroclimatic changes of the past, present, and future (Delavau et al., 2015; Sjostrom and Welker, 2009; Terzer-Wassmuth et al., 2021; Vystavna et al., 2020).

Global efforts have been made to gather data on precipitation stable isotopes already in the mid-20th century, in the form of the Global Network for Isotopes in Precipitation (GNIP) (Araguas-Araguas et al., 1996). Soon after, stand-alone stations and regional networks started to

* Corresponding author.
E-mail address: jan.gacnik@ijs.si (J. Gačnik).

https://doi.org/10.1016/j.envres.2025.123286
Received 30 September 2025; Received in revised form 5 November 2025; Accepted 5 November 2025
Available online 5 November 2025

emerge, such as those in Germany (Stumpp et al., 2014), Switzerland (Schürch et al., 2003), the US (Dutton et al., 2005; Vachon et al., 2010; Welker, 2000, 2012), Canada (Birks and Edwards, 2009), Austria (Hager and Foelsche, 2015), and Australia (Hollins et al., 2018). During the 1960s and 1970s, precipitation stable isotope data have been collected at several locations across central and SE Europe (Argiriou and Lykoudis, 2006; Gospodarič and Habič, 1976).However, systematic monitoring in the region was only initiated in the early 1980s (Krajcar Bronić et al., 1998; Pezdič, 1999, 2003). Some of the established monitoring stations hold remarkably long observation records, yet recurring multi-monthly gaps pose challenges for the analysis of trend and cyclic components (Krajcar Bronić et al., 2020a, 2020b). Quasi-continuous multi-decadal precipitation stable isotope records have also been obtained at two stations in Slovenia, Portorož and Ljubljana, now spanning 24 and 43 years of monthly precipitation stable isotope observations, respectively (Vreča and Malenšek, 2016).

Analysis of 21 long-term GNIP data series of δ^{18}O variability in precipitation revealed complex and diverse isotopic patterns and trends that cannot be simplistically linked to climate type or generalized notions such as *climate change*. Instead, the long-term global δ^{18}O variability likely reflects the sensitivity to a range of regional and global hydroclimatic processes, which are not easily unified in time or space without continuous or higher-frequency isotope monitoring. Furthermore, urbanization has been shown to significantly impact local climate systems, with urban heat islands influencing temperature and precipitation patterns, and these effects further complicate the interpretation of regional isotopic data (Carton et al., 2024).

Despite the growing body of work, multidecadal stable isotope records from SE Europe were not included in the most recent global assessments of long-term isotope trends (Vystavna et al., 2020). This represents a significant gap, as Central and SE Europe is characterized by distinctive hydroclimatological conditions, receiving moisture from two major marine sources: the Atlantic Ocean and the Mediterranean Sea, and experiencing large seasonal variability in contribution from terrestrial moisture recycling (Ciric et al., 2018; Gõmez-Hernández et al., 2013; Krklec et al., 2018). Due to these circumstances, assessing the trends and cyclic components of multidecadal precipitation stable isotope records in SE Europe could offer valuable insights.

The main aims of this study are to: i) identify nonlinear and nonstationary processes embedded in isotopic records using a time series decomposition method (Huang and Wu, 2008); ii) test the hypothesis that the seasonal and decadal-scale oscillatory components of the long-term stable isotope records from Ljubljana are driven by distinct hydroclimatic processes; iii) evaluate the impact of changes in air mass origin, particularly the contribution of Mediterranean-sourced moisture, on isotopic variability; and iv) assess the regional relevance of the findings by comparing results with isotope records from a costal site (Portorož, Slovenia) and a continental site (Vienna, Austria).

2. Materials and methods

2.1. Isotopes in precipitation and meteorological data

Due to its position in temperate latitudes, strong diversity of landforms and differences in heights at the transition of the Alps to the Dinaric range and of the Mediterranean to the Pannonian Basin (Fig. 1), Slovenia has a transitional type of climate, which results from the interaction between maritime and continental air masses (Ogrin, 2015). Consequently, there are interactions between the mountain (Alpine), Mediterranean and continental (Pannonian) climates in Slovenia, as discussed in our previous work (Vreča et al., 2006, 2008, 2011, 2014, 2015, 2022).

A dataset of 997 monthly precipitation δ^2H and δ^{18}O records was collected from Ljubljana (Table 1) for the period May 1981–December 2024. The records were obtained from different publicly available sources, including the Slovenian Network of Isotopes in Precipitation (SLONIP) (Jožef Stefan Institute, 2020; Kern et al., 2020; Vreča et al., 2008, 2014, 2022; Vreča and Malenšek, 2016). Additional, new isotope data were collected from the Jožef Stefan Institute's archive and merged into complete datasets (Supporting Information, "Supplemental Data Ljubljana"). For comparison within a wider geographical area, precipitation stable isotope data for two reference stations were also investigated. These data were collected for coastal station Portorož in Slovenia (Table 1) for the period October 2000–December 2024 and continental station Vienna in Austria for the period January 1973–December 2023 (Table 1, Fig. 1). All together 568 δ^2H and δ^{18}O data were collected for Portorož from publicly available sources, including the SLONIP (Jožef Stefan Institute, 2020), and other sources (Kern et al., 2020; Vreča et al., 2011, 2015, 2022; Vreča and Malenšek, 2016), merged into complete datasets (Supporting Information, "Supplemental Data Portoroz"). The 1189 δ^2H and δ^{18}O data for Vienna were collected form Global Network of Isotopes in Precipitation (GNIP) (International Atomic Energy Agency and World Meteorological Organization) and the Austrian Network of Isotopes in Precipitation (Bundesministerium für Land-und

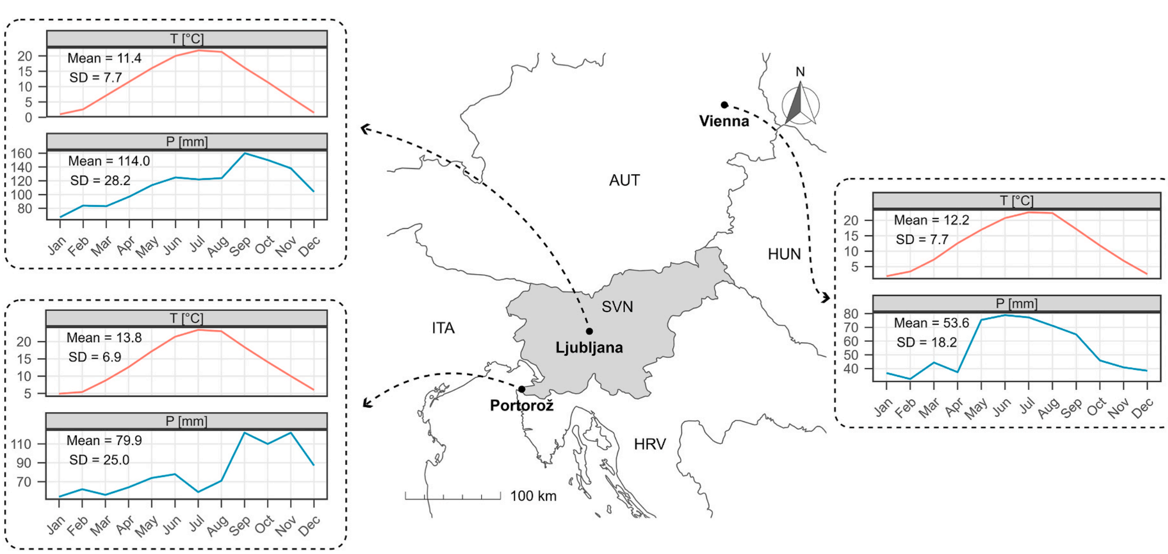

Fig. 1. Map indicating the location of Ljubljana and nearby station with available long-term precipitation isotopic data (marked with black dots). Three letter country codes follow the ISO 3166 alpha-3 system. Climate plots are provided for each of the corresponding station.

Table 1
Basic station attributes. Climate code – Köppen-Geiger classification (Kottek et al., 2006), n.a. – not applicable, JSI – Jožef Stefan Institute, 1 – The data for the Ljubljana stations are merged into a single dataset.

Station ID	Station Name	Lat	Lon	Altitude	Climate code	Data period		Number of isotope data
		° N	° E	m		since	to	
SLO_01	Ljubljana–Bežigrad[1]	46.065507	14.512352	299	Cfb	05/1981	12/1992	997
SLO_02	Ljubljana–JSI[1]	46.041944	14.487778	292		01/1993	08/2000	
SLO_03	Ljubljana–Reaktor[1]	46.094612	14.597046	282		09/2000	12/2024	
SLO_04	Portorož	45.475314	13.615985	2	Cfa	10/2000	12/2024	568
n.a.	Vienna (Hohe Warte)	48.248611	16.356389	198	Cfb	01/1973	12/2023	1189

Forstwirtschaft) (Supporting Information, "Supplemental Data Vienna").

The collected stable oxygen (δ^{18}O) and hydrogen (δ^{2}H) isotope data are expressed in standard δ notation, as per mil (‰) deviation of the sample (*sp*) from the standard (*st*) as:

$$\delta^{y}X\ (‰) = \left(\frac{R_{sp}}{R_{st}}\text{-}1\right) \times 1000 \tag{1}$$

where ${}^{y}X$ is ^{2}H or ^{18}O, R_{sp} and R_{st} is ^{2}H/^{1}H or ^{18}O/^{16}O ratio of the sample and the standard, respectively (Coplen, 1995). Measurements were carried out together with laboratory reference materials that are calibrated periodically against International Atomic Energy Agency (IAEA) calibration standards to VSMOW/SLAP international reference scale (International Atomic Energy Agency and World Meteorological Organization; Lancaster et al., 2025; Vreča et al., 2022, 2015, 2014, 2011, 2008; Vreča and Malenšek, 2016), ensuring comparability and joint assessment of the data. The final δ^{18}O and δ^{2}H data are rounded to 2 decimals and 1 decimal, respectively. The performance of the methods used was regularly tested with participation in IAEA's Water Isotope Inter-laboratory Comparisons (Wassenaar et al., 2018), other inter-laboratory tests, and regular use of commercial reference materials from USGS. Analytical methods have changed over time, as described in detail in the referenced works (International Atomic Energy Agency and World Meteorological Organization; Vreča et al., 2022, 2015, 2014, 2011, 2008; Vreča and Malenšek, 2016). Typical analytical precisions (given as 1σ) for the datasets until 2016 were 0.10 ‰ and 1.0 ‰ for δ^{18}O and δ^{2}H, respectively. In 2016 the infrastructure of the JSI laboratories was improved and the overall uncertainties are estimated to be less than 0.05 ‰ and 1 ‰ for δ^{18}O and δ^{2}H (Vreča et al., 2022). Deuterium excess was calculated as *d*-excess $= \delta^{2}\text{H} - 8 \times \delta^{18}\text{O}$ (Dansgaard, 1964) and reported in ‰ to 1 decimal.

Monthly precipitation and mean monthly air temperature date were acquired from the Ljubljana-Bežigrad and Portorož airport meteorological stations, which are part of the Slovenian National Meteorological Network maintained by the Slovenian Environmental Agency (Slovenian Environmental Agency (ARSO), 2025).

The monthly data were pre-processed for spatial consistency by comparing to coinciding observations available from adjacent sites via an outlier detection method combining both density and distance aspects (Erdélyi et al., 2024) using an on-line web-app (Hatvani et al., 2026). No regionally inconsistent values were found in the records during the procedure; thus, the whole time series were used in the further analyses. The gaps in the time series caused by the missing monthly δ^{18}O and δ^{2}H values were filled by calculating the regional mean of altitude-corrected precipitation isotope values from nearby stations identified within a 100 km radius (δ^{18}On and δ^{2}Hn in Supporting Information). The altitude correction was applied based on region-specific gradients of -1.2 ‰ km^{-1} for δ^{18}O and -7.9 ‰ km^{-1} for δ^{2}H (Hatvani et al., under review; Kern et al., 2020). The imputation uncertainty amounted to ~0.1 (1σ) and ~0.8 (1σ) for δ^{18}O and δ^{2}H, respectively, and was generally lower than the analytical uncertainty.

Descriptive statistics (mean, median, quartiles, and range) and data visualization was done in R version 4.4.2 (R Core Team, 2021). Precipitation-weighted and unweighted 10-year rolling averages of isotopic variables were obtained using the "slider" package (Vaughan, 2024), where the following equations were used for unweighted and weighted means (x_i and p_i are the isotopic variable and the total precipitation amount for a particular month, respectively, and n is the number of total observations in the particular rolling window):

$$\bar{x}_{unweighted} = \frac{\sum_{i=1}^{n} x_i}{n} \tag{2}$$

$$\bar{x}_{weighted} = \sum_{i=1}^{n} x_i w_i \ ; \ w_i = \frac{p_i}{\sum_{i=1}^{n} p_i} \tag{3}$$

Post-processing of figures and creation of the graphical abstracts were done in Inkscape version 1.4. The outline of the overall data analysis approach with corresponding methods used is shown in Fig. S1. All data analysis and visualization scripts are available at the GitHub repository (https://github.com/jgacnik/Precipitation_isotopes_data_analysis).

2.2. Trend analysis

The presence of significant ($p < 0.05$) monotonic trends for δ^{18}O, δ^{2}H, and *d*-excess time series were explored using Sen's slope test (Sen, 1968) and their significance assessed using the Mann-Kendall nonparametric test (Kendall, 1975; Mann, 1945) using the "trend" package. Prior to applying the Mann–Kendall and Sen's slope tests, the raw data were aggregated to annual means to minimize the influence of seasonal variability and to focus the analysis on long-term trends. The statistical evaluation of seasonality for isotopic variables was done using the nonparametric Kruskal-Wallis test in combination with post-hoc analysis using the pairwise Mann-Whitney U tests. All statistical tests were taken as significant at the $a = 0.05$ level.

2.3. Trend decomposition

Time series were decomposed by using i) ensemble empirical mode decomposition (EEMD) to decompose the signal into multiple single modes, also known as intrinsic mode functions (IMFs), and ii) Hilbert spectral analysis for obtaining and analysing the time-frequency spectra of generated IMFs (Huang et al., 1998).

Briefly, the EEMD decomposes time series data ($x(t)$) into a series of oscillating functions ($IMF_i(t)$) and a residual ($r(t)$), through the following equation:

$$x(t) = \sum_{i=1}^{n} IMF_i(t) + r(t) \tag{4}$$

where the decomposition is stopped once the standard deviation between two successive oscillatory components (sifted components) falls below a predefined threshold (typically between 0.2 and 0.3), ensuring that each IMF has a locally zero mean and that the number of local maxima and minima is equal or differs by at most one (Huang et al., 1998). The standard deviation criterion is dimensionless and reflects the relative change between two successive siftings. Additionally, EEMD repeats the process multiple (typically 50–150) times, hence the name "ensemble", with added Gaussian noise, and the mean IMFs produced as the final result (Huang and Wu, 2008). In this work, we used the package

"Rlibeemd" for EEMD analysis (Luukko et al., 2016) and values of 0.2 and 100 for the threshold and the ensemble, respectively. Both the S-number and the maximum number of siftings were used as the stopping criteria for the EEMD procedure. This means that the iterations stopped either when: i) the number of extrema and zero crossings in the signal differed at most by one and stayed the same for S consecutive iterations, or ii) the number of iterations exceeded the maximum number of siftings (Luukko et al., 2016). In the present work, the maximum number of iterations was defined as 50, and S was set to 4. The EEMD requires a continuous time series to identify local extrema for extracting IMFs. Missing data can disrupt this process, so data gaps in the time series of precipitation isotope data for Ljubljana (approximately 5 % of time points) were filled by using the average values of nearby stations with available precipitation data. Gap-filling was necessary to meet the method's requirement for a continuous signal. The small proportion of imputed data was considered acceptable for this analysis.

The statistical significance of EEMD-derived IMFs was evaluated using a Monte Carlo approach. For each variable, 1000 surrogate Gaussian white noise series (matching the original series in length and variance) were decomposed via EEMD with the same parameters. IMF variances from the original data were compared to corresponding surrogate distributions to estimate probabilities; IMFs with $p < 0.05$ were deemed significant, indicating non-random oscillatory components.

Finally, the IMFs were transformed using Hilbert-Huang transform (HHT) to obtain amplitude envelopes, thus providing a different expression of the $x(t)$ using the instantaneous amplitude ($a_i(t)$) and phase ($\theta_i(t)$) of the IMF:

$$x(t) = \sum_{i=1}^{n} a_i(t) \cos \theta_i(t) + r(t) \quad (5)$$

The HHT was done using the "gsignal" package (Van Boxtel et al., 2021). Each IMF was further analyzed using Fourier transform to extract its frequency components. The resulting power spectrum revealed dominant oscillation periods, revealed the periodic structure of the signal and enabled identification of the dominant oscillation period associated with each IMF.

The procedure outlined above is described in greater detail in Nguyen et al. (2022), with the exception of the determination of IMF significance, which was assessed using a Monte Carlo approach in the present study. The approach has been utilized for decomposition of various geophysical and environmental signals, but not for precipitation stable isotope records, separating the signal into meaningful components that show short-term fluctuations, seasonal patterns, and long-term trends (Chen et al., 2025; Nguyen et al., 2022; Wang et al., 2015; Yang et al., 2024; Zhang et al., 2024).

2.4. Long term covariance of δ^2H and δ^{18}O

The linear relationship between δ^2H and δ^{18}O in precipitation, known as the meteoric water line, is a fundamental hydrological concept (Gat, 2005). The local meteoric water line (LMWL) represents the best-fit line through δ - δ space for precipitation at a specific site. In the present case, the LMWLs were calculated using major axis regression (MA), reduced major axis regression (RMA), precipitation weighted MA (PWMA), and precipitation weighted RMA (PWRMA) following the suggestions in refs (Crawford et al., 2014; Hughes and Crawford, 2012). The formulation of the regressions is described in more detail in the framework of the SLONIP platform (Vreča et al., 2022).

2.5. Circulation

To semi-quantitatively assess whether decadal change of Mediterranean-sourced air masses could contribute to the isotopic composition of precipitation in Ljubljana, Hybrid Single-Particle Lagrangian Integrated Trajectory (HYSPLIT) analysis was used (Draxler and Hess, 1997; Stein et al., 2015). 6-hour back trajectories of air parcels arriving at the Ljubljana, Portorož, and Vienna stations were calculated for the periods 1981–2024, 2000–2024, and 1973–2023, respectively, using the following input parameters: 3000 m above sea level as the top of the model and −120 h as the total run time. For meteorological data, National Center for Environmental Prediction (NCEP) - National Center for Atmospheric Research (NCAR) reanalysis data were used, specifically the "NCEP-NCAR reanalysis I" data provided by the NOAA PSL, Boulder, CO, USA (Kalnay et al., 1996), from their website (https://psl.noaa.gov). To link the back trajectories to the Mediterranean Sea, we used the Mediterranean Sea geographical polygon as defined by the International Hydrographic Organization (IHO) (Flanders Marine Institute, 2018) and the R package "sf" (Pebesma, 2018). The time points of the trajectories that fell within the Mediterranean Sea polygon were compared with the total number of trajectory points for the investigated period to obtain the percentage of Mediterranean-origin air masses. The trajectories of air masses for the days without precipitation in Ljubljana, Portorož, and Vienna were filtered out based on historical daily precipitation data obtained from the Slovenian Environmental Agency (Ljubljana and Portorož) (Slovenian Environmental Agency (ARSO), 2025) and GeoSphere Austria (Vienna) (Geosphere Austria).

While this approach provides useful insights into air mass origins, it does not directly model the transport of water vapor. Ideally, an atmospheric model that simulates water molecules directly would be used (Sodemann et al., 2008; Stohl et al., 2005), but such modelling was beyond the scope of this study.

Beside this semi-quantitative measure of the proportion of Mediterranean-sourced air masses, two oscillation indices were also tested as potential indicators of changes in air-mass origin in the study area. The North Atlantic Oscillation (NAO) represents the atmospheric pressure gradient between the Azores High and the Iceland Low (Hurrell, 1995). The NAO reflects the intensity of westerly circulation between these latitudes, and the hydroclimatic sensitivity of the Euro-Mediterranean region to NAO variability and forcing is well-known (Hurrell, 1995; López-Moreno and Vicente-Serrano, 2008; Trigo et al., 2002). In this study, the NAO index was defined using principal component analysis of the Northern Hemisphere 500 mb fields (Barnston and Livezey, 1987). The monthly mean NAO index series for period 1950–2024 was obtained from the NOAA Climate Prediction Centre website (https://www.cpc.ncep.noaa.gov/products/precip/CWlink/pna/nao.shtml). The Mediterranean Oscillation (MO) index was defined as the normalized pressure difference between Algiers (36.4°N, 3.1°E) and Cairo (30.1°N, 31.4°E.) (Palutikof et al., 1996). Although the MO is not independent of the NAO, it has been proven to be a reliable measure of atmospheric forcing over the Mediterranean Basin, since on an annual basis it provides a stronger correlation with the main climatic variables that influence freshwater and heat budgets in the region (Criado-Aldeanueva et al., 2014; Kutiel and Maheras, 1998). The obtained time trend was statistically evaluated using methodologies described in sections 2.2 and 2.3.

3. Results and discussion

In the Ljubljana dataset, the medians and interquartile ranges of the monthly values of δ^{18}O, δ^2H, *d*-excess, temperature, and precipitation amount are −8.0 ‰ (−10.4 to −6.4), −54.0 ‰ (−72.3 to −41.3), 10.0 ‰ (8.0–11.9), 11.2 °C (4.5–17.9), and 107.0 mm (64.8–150.3), respectively; full summary of descriptive statistics can be found in Table S1.

3.1. Time trends and seasonality

10-year rolling averages indicate visually increasing trends for δ^{18}O, δ^2H, and *d*-excess over time (Fig. 2a). These increases are further supported by statistical analyses of the yearly averaged raw data, which reveal significant increasing trends on for all variables ($p = 0.050$ for δ^{18}O, $p = 0.0097$ for δ^2H, and $p < 0.001$ for *d*-excess). However, the δ^{18}O

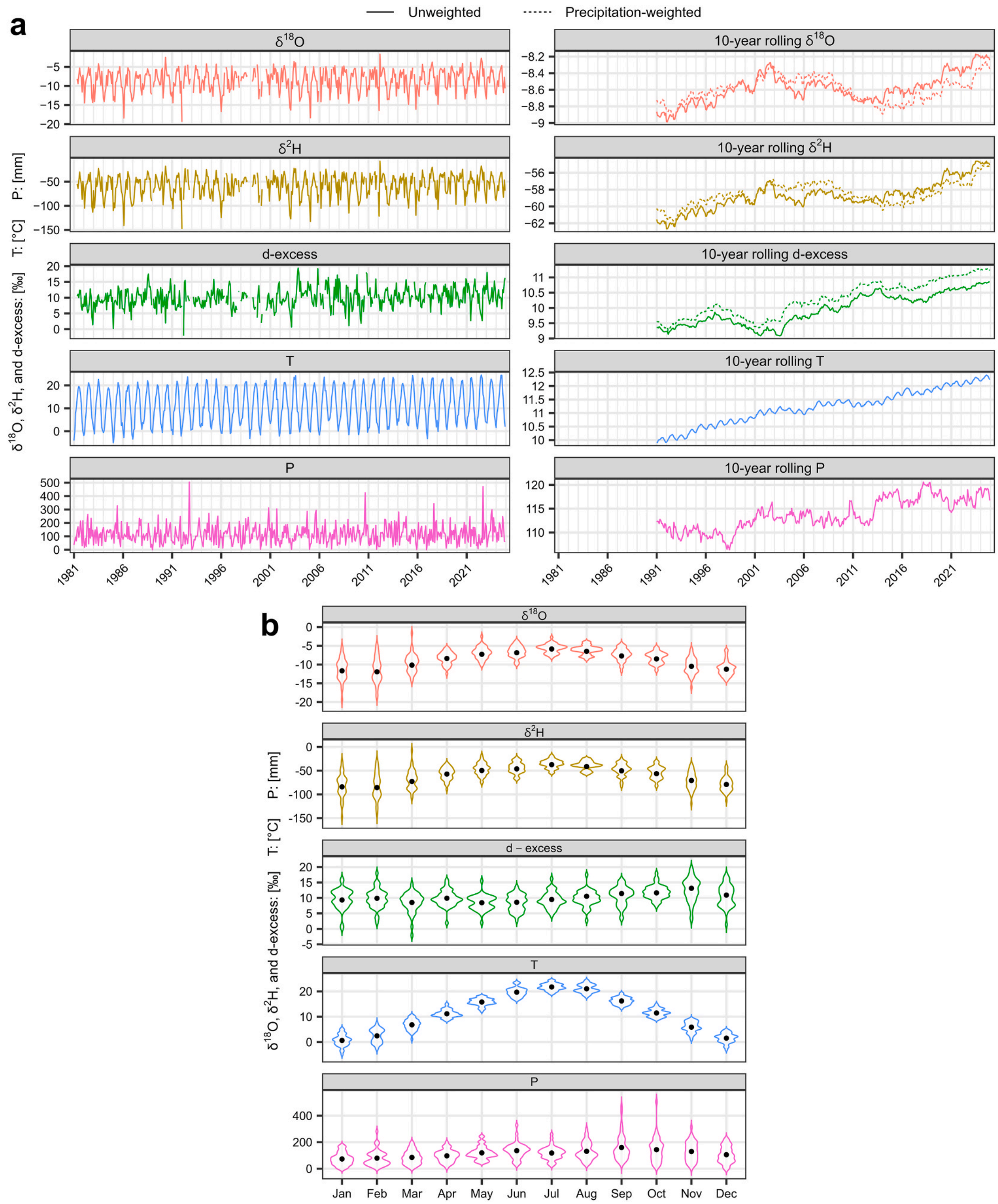

Fig. 2. a) Raw values and 10-year rolling averages of isotopes in precipitation and related meteorological variables in Ljubljana. b) Monthly variation of all variables indicated on violin plots, where dots indicate the mean value (Hintze and Nelson, 1998).

trend was only marginally significant. Sen's slope estimates for yearly averaged data indicate that the rate of monotonic change is +0.02 ‰ yr^{-1} for $\delta^{18}O$, +0.18 ‰ yr^{-1} for δ^2H, and +0.05 ‰ yr^{-1} for *d*-excess. The yearly average air temperature also shows a significant increasing trend ($p < 0.001$), with a Sen's slope of +0.069 °C yr^{-1}, whereas no significant monotonic trend is observed for the yearly average precipitation amount ($p = 0.32$).

Regarding the seasonal distribution of $\delta^{18}O$ values (Table S2; winter: Dec–Feb, spring: Mar–May, summer: Jun–Aug, autumn: Sep–Nov), there is a statistically significant difference between all pairs of seasonal $\delta^{18}O$ data ($p < 0.001$) except for the spring-autumn pair ($p = 0.23$). A similar pattern is observed for δ^2H data. The seasonality patterns of $\delta^{18}O$ and δ^2H data match the seasonality pattern of temperature, a well-known phenomenon for isotopes in precipitation (Salamalikis et al., 2016a).

More interestingly, there is a statistically significant difference in *d*-excess between autumn and all other seasons ($p < 0.001$), while there is no significant difference between other season pairs. This indicates that autumn is the season with the most unique and highest *d*-excess values for Ljubljana. Autumn is also the season with the highest and the most variable precipitation amount of all seasons (Fig. 2b). Values by month (Fig. 2b, Table S3) show a similar trend as the seasonal plots. Notably, September, October, and November are the only months that showed significantly different *d*-excess values compared to other months (Table S4). Among them, November appears to be the most unique month with respect to *d*-excess in Ljubljana. These findings are consistent with similar observations in the Central Mediterranean, such as those in Pisa, Italy (Natali et al., 2025).

The trends of δ^2H versus $\delta^{18}O$ regressions suggest that slopes and intercepts for precipitation in Ljubljana are decreasing (Fig. 3), regardless of the used regression method or weighting. A similar decreasing trend is also observed when splitting data into decades (Fig. S2). This pattern may be the result of two main factors: i) rising temperatures

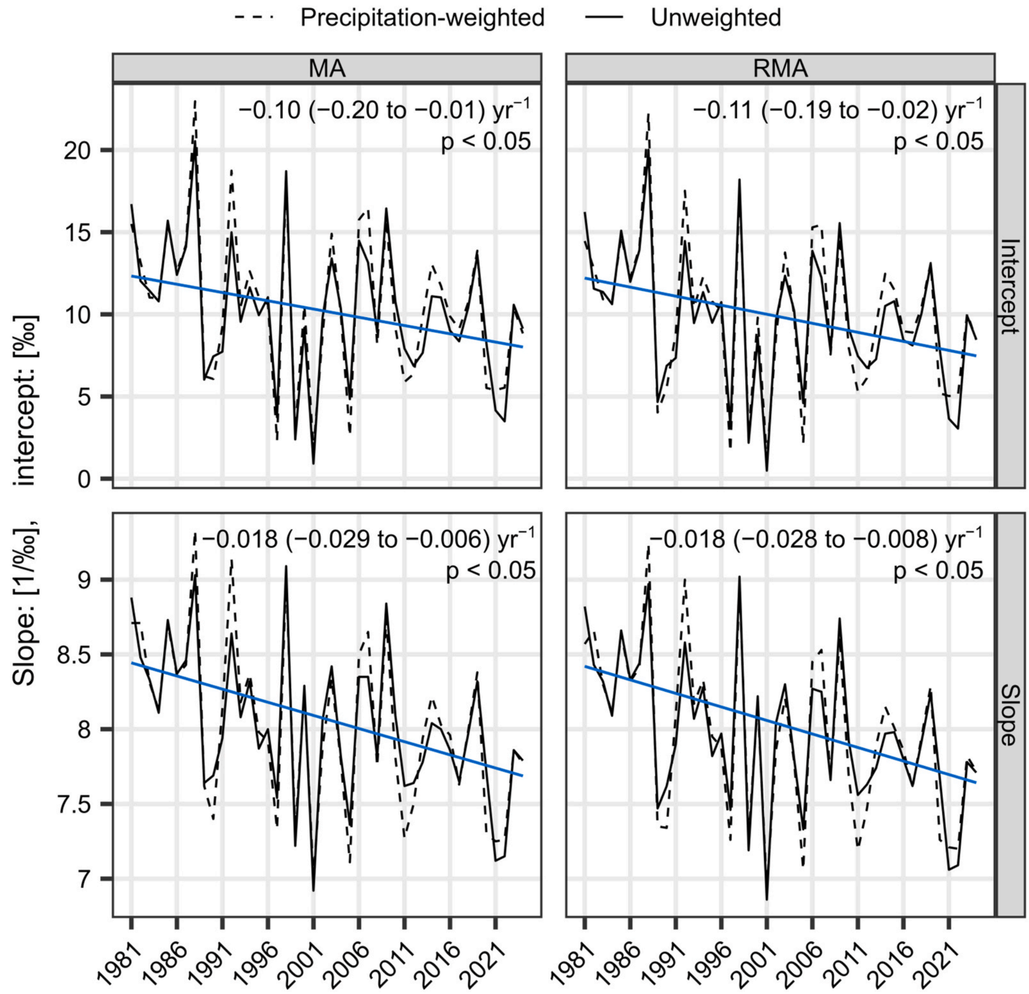

Fig. 3. The change of yearly regression coefficients and intercepts for the δ^2H versus δ^{18}O plots. The straight blue lines represent Sen's slope linear regressions. RMA and MA stand for reduced major axis and major axis regressions. Values in brackets correspond to the 95 % confidence interval. (For interpretation of the references to colour in this figure legend, the reader is referred to the Web version of this article.)

(Fig. 2), which increase evaporative processes and promote moisture recycling, both of which lead to isotopic enrichment of precipitation (Salamalikis et al., 2016b); and/or ii) temporal shifts in the water vapor sources. In particular, the Mediterranean Sea is a well-known moisture source for this region (Ciric et al., 2018; Gõmez-Hernández et al., 2013) and is typically associated with higher δ^{18}O and δ^2H values compared to Atlantic-derived air masses (Gat et al., 2003). These two contributing factors are explored in more detail below.

3.2. *Time series decomposition*

The decomposition of δ^{18}O, δ^2H, and *d*-excess time series reveals significant oscillations through EEMD-derived IMFs and corresponding instantaneous frequencies and amplitudes obtained from HHT analysis. The decomposition highlights temporal patterns in the data (Fig. 4a). The dominant oscillation periods were determined via spectral analysis, as exemplified by IMF 3 for *d*-excess (Fig. 4b; full spectral analysis in Fig. S3). The strongest oscillations with the highest mean amplitudes were the 1-year oscillations for all variables: δ^{18}O (3.18 ‰, IMF 2 + IMF 3), δ^2H (25.17 ‰, IMF 2 + IMF 3), and *d*-excess (1.83 ‰, IMF 3). The decomposition residuals, representing the long-term non-periodic component remaining after removal of cyclical trends, provide insight into baseline processes influencing the source and transport of moisture. These residuals show a steady increase with time for all variables, in agreement with the observed 10-year rolling averages (Fig. 2a). Since the 1-year oscillations were also significant for temperature (T) and precipitation amount (P) ($p < 0.001$), correlations between these variables and the yearly δ^{18}O, δ^2H, and *d*-excess were analyzed (Fig. 4c, Table S6). Strong positive correlations (r > 0.6) were found for 1-year oscillations (IMF 2) of δ^{18}O and δ^2H with T, confirming that these variables follow the annual temperature cycle (Fig. 4b). Decomposition residuals of all variables were strongly correlated (r > 0.8) with both P and T, reflecting the increasing long-term values in all decomposed variables. Initially, no strong correlation was observed between the *d*-excess oscillations and the T/P oscillations. However, cross-correlation analysis (Fig. S4, Text S1) revealed a time lag of approximately two months between the 1-year cycles of temperature and *d*-excess (Fig. 4c). A moderate cross-correlation (> 0.4) was observed between the annual temperature and *d*-excess cycles. The correlation could have been stronger, but the time lag was not consistent throughout the study period. Up to around 1990, the oscillations were largely in phase, whereas after that point, the lag became more apparent (Fig. 4c). Nonetheless, this correlation does not extend to the longer-term *d*-excess oscillations (IMF 4 and IMF 5), suggesting that neither temperature nor precipitation is the dominant driver of these components. This was further investigated in Section 3.3.

The observations from time series decomposition for Ljubljana were further explored on two additional nearby long-term datasets, from the Portorož and Vienna stations (Fig. 1, Table 1). The most powerful oscillations from the decomposition of Porotož and Vienna datasets were

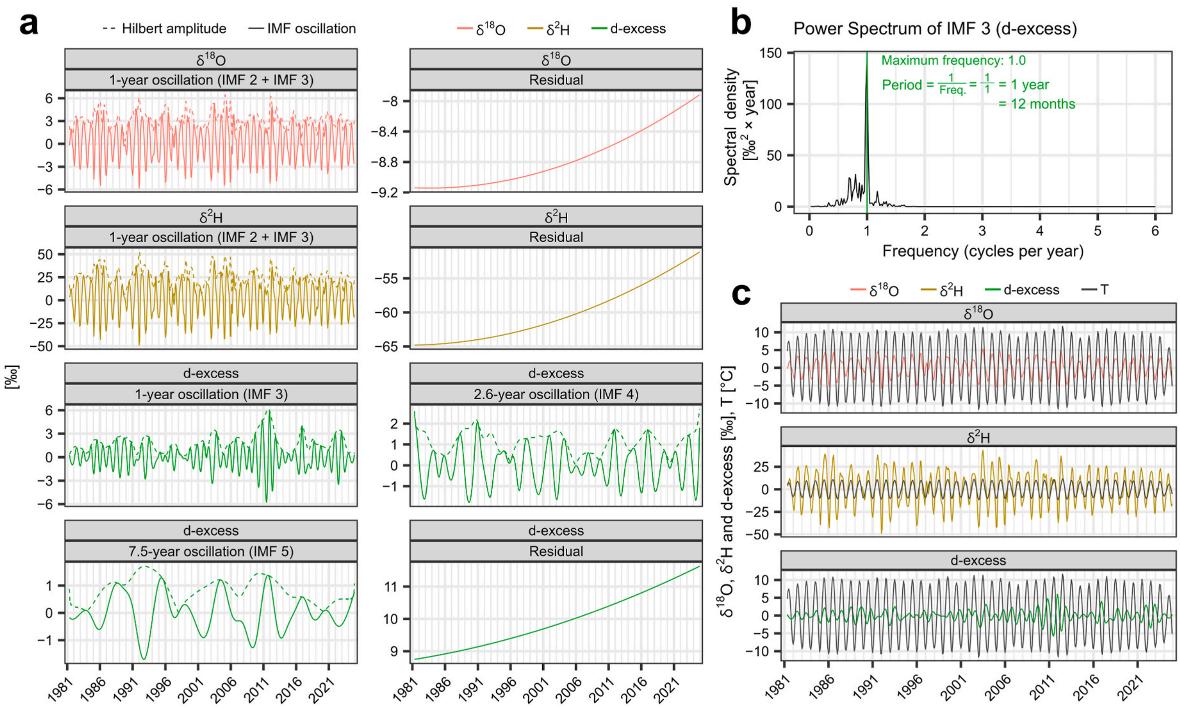

Fig. 4. a) Ensemble empirical mode decomposition (EEMD) of δ^{18}O, δ^{2}H, and *d*-excess time series into intrinsic mode functions (IMFs) and residual with corresponding amplitude envelopes from Hilbert-Huang transform. Each IMF number represents a statistically significant oscillation at different time scales. b) Power spectral density of IMF 3 for *d*-excess data, showcasing the calculation of the oscillation period. c) Overlapping of the 1-year oscillations of δ^{18}O, δ^{2}H, and *d*-excess with the 1-year temperature oscillation. The full list of IMFs and decomposition results is provided in Table S5, while the explanation on the merging of oscillations (e.g., IMF 2 + IMF 3) is provided in Text S1.

the 1-year oscillations for δ^{18}O, δ^{2}H, and *d*-excess; all of them correlated with the 1-year oscillation of temperature (Table S6, Table S7). There is a time lag between the 1-year cycles of temperature and *d*-excess, namely a 2-month lag for Portorož and a 3-month lag for Vienna, similar to the observed time lag for Ljubljana. The correlations with temperature are weaker for Portorož, which can be related to the lower isotopic amplitude at this coastal station/maritime conditions similarly to the findings on Central European precipitation δ^{18}O records (Salamalikis

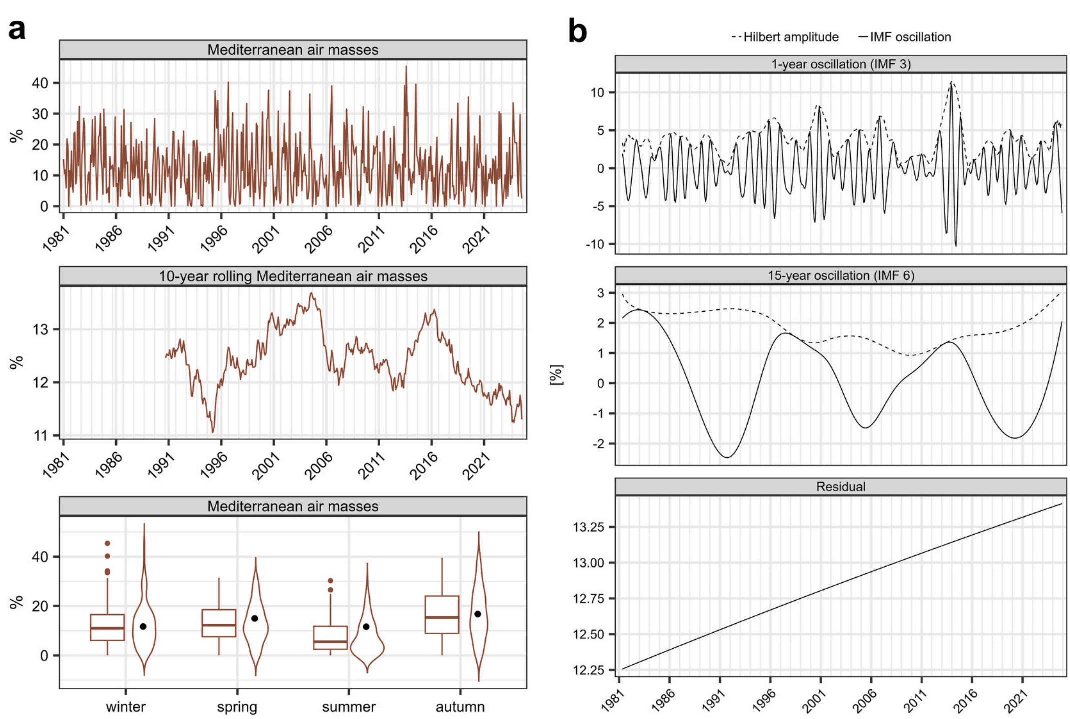

Fig. 5. a) Time series, 10-year rolling averages, and seasonality of Mediterranean-sourced air masses in Ljubljana. b) Ensemble empirical mode decomposition (EEMD) of the Mediterranean-sourced air masses time series into intrinsic mode functions (IMFs) and a residual with corresponding amplitude envelopes from Hilbert-Huang transform. Only significant IMFs are shown.

et al., 2016a; Vreča et al., 2006). Overall, Portorož and Vienna results are in agreement with the decomposition results of the Ljubljana dataset, suggesting that the observations are not only local, but relevant to a wider regional scale. The lower-frequency IMFs of *d*-excess, 2.7-year and 7.5-year oscillations, seem to be less relevant at the coastal Portorož site ($p = 0.07$ and $p = 0.37$, respectively) while their significance increases ($p = 0.01$ and $p < 0.001$, respectively) with increased continental character of the station (e.g., Vienna).

3.3. Connection to the mediterranean

Trajectories of HYSPLIT-derived time series of back trajectory points in Ljubljana, crossing the Mediterranean region during their travel, are shown in Fig. S5. The percentage of air masses originating from the Mediterranean Sea ranges from 0 to 45 % in Ljubljana on the monthly basis, and 10-year rolling averages are decreasing (Fig. 5a), with a Sen's slope of −0.046 % (−0.053 to −0.40) yr^{-1}. Since a decrease in the contribution of Mediterranean-sourced air masses would, if anything, decrease the *d*-excess values, the increasing long-term values for *d*-excess in Ljubljana are most likely not caused by changes in the contribution of Mediterranean-sourced air masses. This is particularly evident considering that Mediterranean-sourced vapor typically imprints high *d*-excess values (Gat and Carmi, 1970), higher relative to Atlantic-sourced moisture (Bottyán et al., 2017). However, the seasonality of these air masses (Fig. 5a: bottom plot) clearly shows autumn is the season with the highest percentage of air masses arriving to Ljubljana from the Mediterranean Sea, driving the seasonal variability of *d*-excess (Fig. 2b).

From the time series decomposition, the strongest IMF with the mean amplitude of 3.8 % was IMF 3, having a 1-year dominant oscillation period (Fig. 5b; full decomposition results in Table S8). This seasonal oscillation is most likely linked to the seasonality of *d*-excess; however, it is not correlated to any of the significant oscillations of *d*-excess (Table S9), even when checking for phase shifts between oscillations. The lower frequency oscillation, IMF 6, had a 15-year dominant period of oscillation and an amplitude of 1.7 % (Fig. 5b). Again, this oscillation is not strongly or moderately correlated to any of the significant oscillations of *d*-excess (Table S9). The decomposition residual shows an increase with time (Fig. 5b), in disagreement with the observed 10-year rolling averages (Fig. 5a). The residual of Mediterranean air masses increased by 1 % during the period, which represents an 8 % relative increase since 1981. This is a small increase in comparison to the 52 % relative increase of *d*-excess residual since 1981 (absolute increase of 4.6 ‰), which suggests that Mediterranean-origin air masses are not the sole driver of long-term *d*-excess values in Ljubljana.

Overall, the statistical evaluation of the decomposition of the HYSPLIT-derived time series suggests that temporal changes in the contribution of Mediterranean-sourced air masses are not the primary driver of the long-term increase in *d*-excess values in Ljubljana. A similar observation was found for a Central European precipitation site, where $\delta^{18}O$ showed no dependence on air mass sources, but rather on evaporative processes and moisture recycling (Krklec et al., 2018). Although the Mediterranean influence shows a clear seasonal pattern, particularly with higher contributions in autumn, it does not explain the observed long-term trend. The absence of correlation between the dominant low-frequency oscillations of Mediterranean-sourced air masses and those of *d*-excess further supports this conclusion. However, the seasonal variability in the origin of air masses, especially the increased autumn input from the Mediterranean Sea, appears to play an important role in shaping the seasonal cycle of *d*-excess in Ljubljana.

Using the same HYSPLIT-based approach for the nearby stations of Portorož and Vienna also reveals characteristically elevated *d*-excess values during autumn (Fig. S6), which is consistent with observations from neighbouring regions where precipitation *d*-excess tends to peak in the fall (Masiol et al., 2021). As with Ljubljana, the temporal decomposition of Mediterranean-sourced air mass contributions at these sites does not exhibit significant correlation with the low-frequency oscillations of *d*-excess (Tables S8 and S11). This consistency across multiple locations reinforces the conclusion that these findings are not only local, but relevant across the region. Moreover, the lack of correlation between *d*-excess and Mediterranean-origin air masses aligns with previous studies; for instance, isotope monitoring in Austria has shown that large *d*-excess fluctuations are more strongly influenced by local factors (e.g., sub-cloud evaporation, regional circulation) than by the air mass source region (International Atomic Energy Agency (IAEA), 2005).

For oscillations of MO, no significant correlations were found with *d*-excess. However, a weak correlation was observed between NAO IMF 4 (2.7-year oscillation) and *d*-excess IMF 4 (2.6-year oscillation), for both Ljubljana ($r = 0.25$) and Vienna ($r = 0.21$), supporting the link previously detected by linear methods (Baldini et al., 2008; Kern et al., 2019; Vystavna et al., 2020) between precipitation stable isotope records and NAO. The time trend decomposition method applied here, which is capable of identifying nonlinear and nonstationary processes, was able to attribute this relation to a 2–3-yr oscillatory component. For Portorož, no significant low-frequency oscillation of *d*-excess was detected, and thus no correlations could be established.

3.4. Implications

Although increasing trends were more common than decreasing ones for precipitation isotopes, statistically significant trends were observed only in very few cases when temporal trends were studied for isotopic composition of monthly composite precipitation in the period of 1961–2000 at nine stations across southern Central Europe and Eastern Mediterranean (Lykoudis and Argiriou, 2011). The lack of a temporal trend might suggest that, despite the widely reported empirical "temperature effect" in this region (Hager and Foelsche, 2015; Krajcar Bronić et al., 2020a; Vreča et al., 2006, 2014) and the ongoing regional warming (Ogrin, 2015), such signals were still unseen in the noisy precipitation stable isotope composition records. However, the strong positive correlation found at the annual scale and in the long-term trend between temperature and precipitation isotopes at each of the studied stations (Table S6) provides clear evidence that the observed atmospheric temperature increase (i.e., energy input) has already propagated into the water cycle. In this respect, the results clearly imply the regional relevance of a globally coherent water cycle response to temperature change (Konecky et al., 2023). The explanation for the previously reported lack of significant trends in the isotopic composition of precipitation for sites in southern Central Europe and Eastern Mediterranean (Lykoudis and Argiriou, 2011) might be that gaps in the assessed records bias trend detection, or that the changes have strengthened during the past 20 years, which were not included in the earlier study (Lykoudis and Argiriou, 2011). The latter explanation is supported by our findings, which show an increase of 1.2 ‰ in $\delta^{18}O$ and 13.7 ‰ in $\delta^{2}H$ over just 43 years during 1981–2024, as calculated from the oscillation residuals in Fig. 4. These changes are striking when compared with the global average increase of only 0.56 ‰ in $\delta^{18}O$ over a much longer period of 150 years during 1850–2000 (Konecky et al., 2023). and local average increase of 0.65 ‰ in $\delta^{18}O$ and 5.3 ‰ in $\delta^{2}H$ over 38 years during 1980–2018 in Zagreb, Croatia (Krajcar Bronić et al., 2020a). Moreover, the trend resembles exponential rather than linear growth (as evidenced by Fig. S7), with the strongest increases occurring in the last two decades.

Understanding temporal and spatial variations in the amount and mode of precipitation and information regarding the stable isotopic composition is essential. Precipitation represents an integral part of the hydrological cycle, as it is the primary source of surface water and groundwater (Dutton et al., 2005; Jasechko et al., 2016) and understanding of the dynamics between different water cycle components is crucial for sustainable water resource management because climate change, land use changes and human activities impact aquifer recharge, as well as surface and groundwater quality and quantity (Schirmer et al., 2013; Žagar et al., 2024). In comparison to precipitation, the surface water and groundwater isotope patterns are significantly dampened but also change in time. Consequently, mean residence times of surface waters and contribution of local precipitation to groundwater recharge are changed (Jasechko et al., 2016; Žagar et al., 2024). These findings have implications for national strategic planning, including the long-term environmental monitoring programs and construction of water resource infrastructure (e.g., dams and wellfields), particularly in light of increasing air temperature and changing precipitation patterns (Papadimitriou et al., 2016; Žagar et al., 2024).

CRediT authorship contribution statement

Jan Gačnik: Writing – original draft, Visualization, Validation, Software, Investigation, Data curation, Conceptualization. **Klara Žagar:** Validation, Methodology, Investigation, Formal analysis. **István Gábor Hatvani:** Writing – review & editing, Software, Investigation, Data curation, Conceptualization. **Zoltán Kern:** Writing – review & editing, Software, Investigation, Formal analysis, Data curation, Conceptualization. **Polona Vreča:** Writing – review & editing, Supervision, Resources, Project administration, Investigation, Funding acquisition, Formal analysis, Data curation, Conceptualization.

Declaration of competing interest

The authors declare that they have no known competing financial interests or personal relationships that could have appeared to influence the work reported in this paper.

Acknowledgements

This research was funded by the Slovenian Research and Innovation Agency (ARIS; research programs P0-0531, 1999–2003, P1-0143, 2004–2024 and bilateral research project N1-0054, 2016–2018), the International Atomic Energy Agency (CRP F31002, CRP F33024, CRP F31006, RER7013, RER7017, NC SLO7001). We greatly acknowledge the work of J. Pezdič, who initiated monitoring of the isotopic composition of precipitation in Ljubljana, and all colleagues of the JSI and other institutions who participated in the long-term monitoring of precipitation in Slovenia. We also thank three anonymous reviewers for their helpful suggestions.

Appendix B. Supplementary data

Supplementary data to this article can be found online at https://doi.org/10.1016/j.envres.2025.123286.

Data availability

The used raw data is contained within the Supplementary Data.

References

Araguas-Araguas, L., Danesi, P., Froehlich, K., Rozanski, K., 1996. Global monitoring of the isotopic composition of precipitation. J. Radioanal. Nucl. Chem. 205, 189–200. https://doi.org/10.1007/BF02039404.

Argiriou, A.A., Lykoudis, S., 2006. Isotopic composition of precipitation in Greece. J. Hydrol. 327, 486–495. https://doi.org/10.1016/j.jhydrol.2005.11.053.

Bailey, H.L., Klein, E.S., Welker, J.M., 2019. Synoptic and mesoscale mechanisms drive winter precipitation δ^{18}O/δ^{2}H in south-central Alaska. J. Geophys. Res. Atmos. 124, 4252–4266. https://doi.org/10.1029/2018JD030050.

Baldini, L.M., McDermott, F., Foley, A.M., Baldani, J.U.L., 2008. Spatial variability in the European winter precipitation δ^{18}O-NAO relationship: implications for reconstructing NAO-mode climate variability in the Holocene. Geophys. Res. Lett. 35. https://doi.org/10.1029/2007GL032027.

Barnston, A.G., Livezey, R.E., 1987. Classification, seasonality and persistence of low-frequency atmospheric circulation patterns. Mon. Weather Rev. 115, 1083–1126. https://doi.org/10.1175/1520-0493(1987)115<1083:CSAPOL>2.0.CO, 2.

Birks, S.J., Edwards, T.W.D., 2009. Atmospheric circulation controls on precipitation isotope-climate relations in western Canada. Tellus Ser. B Chem. Phys. Meteorol. 61, 566–576. https://doi.org/10.1111/j.1600-0889.2009.00423.x.

Bottyán, E., Czuppon, G., Weidinger, T., Haszpra, L., Kármán, K., 2017. Moisture source diagnostics and isotope characteristics for precipitation in east Hungary: implications for their relationship. Hydrol. Sci. J. 62, 2049–2060. https://doi.org/10.1080/02626667.2017.1358450.

Brenčič, M., Kononova, N.K., Vreča, P., 2015. Relation between isotopic composition of precipitation and atmospheric circulation patterns. J. Hydrol. 529, 1422–1432. https://doi.org/10.1016/j.jhydrol.2015.08.040.

Bundesministerium für Land-und Forstwirtschaft, n.d. The ANIP database [WWW Document]. URL https://wasser.umweltbundesamt.at/h2odb/(accessed 4.2.25).

Carton, C., Barbecot, F., Birks, J., Hélie, J.F., 2024. Improved understanding of the impact of urbanization on the temperature, precipitation, and air quality of major eastern Canadian cities. Urban Clim. 53. https://doi.org/10.1016/j.uclim.2023.101781.

Chen, Y., Zhang, H., You, Y., Zhang, J., Tang, L., 2025. A hybrid deep learning model based on signal decomposition and dynamic feature selection for forecasting the influent parameters of wastewater treatment plants. Environ. Res. 266, 120615. https://doi.org/10.1016/j.envres.2024.120615.

Ciric, D., Nieto, R., Losada, L., Drumond, A., Gimeno, L., 2018. The mediterranean moisture contribution to climatological and extreme monthly continental precipitation. Water (Switzerland) 10. https://doi.org/10.3390/w10040519.

Comas-Bru, L., McDermott, F., Werner, M., 2016. The effect of the East Atlantic pattern on the precipitation δ^{18}O-NAO relationship in Europe. Clim. Dyn. 47, 2059–2069. https://doi.org/10.1007/s00382-015-2950-1.

Coplen, T.B., 1995. Reporting of stable hydrogen, carbon, and oxygen isotopic abundances. Geothermics 24, 707–712. https://doi.org/10.1016/0375-6505(95)00024-0.

Crawford, J., Hughes, C.E., Lykoudis, S., 2014. Alternative least squares methods for determining the meteoric water line, demonstrated using GNIP data. J. Hydrol. 519, 2331–2340. https://doi.org/10.1016/j.jhydrol.2014.10.033.

Criado-Aldeanueva, F., Soto-navarro, F.J., García-Lafuente, J., 2014. Large-scale atmospheric forcing influencing the long-term variability of mediterranean heat and freshwater budgets: climatic indices. J. Hydrometeorol. 15, 650–663. https://doi.org/10.1175/JHM-D-13-04.1.

Dansgaard, W., 1964. Stable isotopes in precipitation. Tellus Dyn. Meteorol. Oceanogr. 16, 436–468. https://doi.org/10.3402/tellusa.v16i4.8993.

Dee, S., Bailey, A., Conroy, J.L., Atwood, A., Stevenson, S., Nusbaumer, J., Noone, D., 2023. Water isotopes, climate variability, and the hydrological cycle: recent advances and new frontiers. Environ. Res. Clim. 2, 022002. https://doi.org/10.1088/2752-5295/accbe1.

Delavau, C., Chun, K.P., Birks, S.J., Welker, J.M., 2015. North American precipitation isotope (δ^{18}O) zones revealed in time series modeling across Canada and northern United States. Water Resour. Res. 51, 1284–1299. https://doi.org/10.1002/2014WR015687.

Draxler, R.R., Hess, G.D., 1997. Description of the HYSPLIT_4 Modeling System.

Dutton, A., Wilkinson, B.H., Welker, J.M., Bowen, G.J., Lohmann, K.C., 2005. Spatial distribution and seasonal variation in ^{18}O/^{16}O of modern precipitation and river water across the conterminous USA. Hydrol. Process. 19, 4121–4146. https://doi.org/10.1002/hyp.5876.

Erdélyi, D., Hatvani, I.G., Derx, J., Kern, Z., 2024. Screening a precipitation stable isotope database for inconsistencies prior to hydrological applications – examples from the Austrian network for isotopes in precipitation. Austrian J. Earth Sci 117. https://doi.org/10.17738/ajes.2024.0014.

Flanders Marine Institute, 2018. IHO Sea Areas version 3.

Gat, J.R., Carmi, I., 1970. Evolution of the isotopic composition of atmospheric waters in the Mediterranean Sea area. J. Geophys. Res. 75, 3039–3048. https://doi.org/10.1029/JC075i015p03039.

Gat, J.R., Klein, B., Kushnir, Y., Roether, W., Wernli, H., Yam, R., Shemesh, A., 2003. Isotope composition of air moisture over the Mediterranean Sea: an index of the air-sea interaction pattern. Tellus Ser. B Chem. Phys. Meteorol. 55, 953–965. https://doi.org/10.1034/j.1600-0889.2003.00081.x.

Gat, J.R., 2005. Some classical concepts of isotope hydrology. In: Aggarwal, P.K., Gat, Joel R., Froehlich, K.F.O. (Eds.), Isotopes in the Water Cycle: past, Present and Future of a Developing Science. Springer, Netherlands, Dordrecht, pp. 127–137. https://doi.org/10.1007/1-4020-3023-1_10.

Geosphere Austria, n.d. GeoSphere Austria data hub [WWW Document]. URL https://data.hub.geosphere.at/(accessed 5.25.25).

Gõmez-Hernández, M., Drumond, A., Gimeno, L., Garcia-Herrera, R., 2013. Variability of moisture sources in the mediterranean region during the period 1980-2000. Water Resour. Res. 49, 6781–6794. https://doi.org/10.1002/wrcr.20538.

Gospodarič, R., Habič, P., 1976. Underground water tracing: investigations in Slovenia 1972-1975. In: International Symposium of Underground Water Tracing. ZRC Sazu - Postojna. Bled, p. 309.

Hager, B., Foelsche, U., 2015. Stable isotope composition of precipitation in Austria. Austrian J. Earth Sci 108, 2–14. https://doi.org/10.17738/ajes.2015.0012.

Hatvani, I.G., Erdélyi, D., Vreča, P., Lojen, S., Žagar, K., Gačnik, J., Kern, Z., n.d. Online screening tool for precipitation stable isotopes records: hybrid distance/density based outlier filtering approach via interactive web application (under review). J. Hydrol.

Hintze, J.L., Nelson, R.D., 1998. Violin plots: a box plot-density trace synergism. Am. Stat. 52, 181–184. https://doi.org/10.1080/00031305.1998.10480559.

Hollins, S.E., Hughes, C.E., Crawford, J., Cendón, D.I., Meredith, K.M., 2018. Rainfall isotope variations over the Australian continent – implications for hydrology and

isoscape applications. Sci. Total Environ. 645, 630–645. https://doi.org/10.1016/j.scitotenv.2018.07.082.
Huang, N.E., Shen, Z., Long, S.R., Wu, M.C., Shih, H.H., Zheng, Q., Yen, N.-C., Tung, C.C., Liu, H.H., 1998. The empirical mode decomposition and the Hilbert spectrum for nonlinear and non-stationary time series analysis. Proc. R. Soc. London. Ser. A Math. Phys. Eng. Sci. 454, 903–995. https://doi.org/10.1098/rspa.1998.0193.
Huang, N.E., Wu, Z., 2008. A review on Hilbert-Huang Transform : method and its applications. Rev. Geophys. 46, 1–23. https://doi.org/10.1029/2007RG000228.1.INTRODUCTION.
Hughes, C.E., Crawford, J., 2012. A new precipitation weighted method for determining the meteoric water line for hydrological applications demonstrated using Australian and global GNIP data. J. Hydrol. 464–465, 344–351. https://doi.org/10.1016/j.jhydrol.2012.07.029.
Hurrell, J.W., 1995. Decadal trends in the north Atlantic oscillation: regional temperatures and precipitation. Science 269, 676–679. https://doi.org/10.1126/science.269.5224.676.
International Atomic Energy Agency (IAEA), 2005. Isotopic Composition of Precipitation in the Mediterranean Basin in Relation to Air Circulation Patterns and Climate, TECDOC Series. INTERNATIONAL ATOMIC ENERGY AGENCY, Vienna.
International Atomic Energy Agency, World meteorological organization, n.d. global network of isotopes in precipitation. The GNIP Database [WWW Document]. URL https://nucleus.iaea.org/wiser (accessed 4.21.22).
Jasechko, S., Kirchner, J.W., Welker, J.M., McDonnell, J.J., 2016. Substantial proportion of global streamflow less than three months old. Nat. Geosci. 9, 126–129. https://doi.org/10.1038/ngeo2636.
Jožef Stefan Institute, 2020. SLONIP: Slovenian network of isotopes in precipitation [WWW Document]. URL. https://slonip.ijs.si/ (accessed 6.10.25).
Kalnay, E., Collins, W., Deaven, D., Gandin, L., Iredell, M., Jenne, R., Joseph, D., 1996. The NCEP NCAR 40-year reanalysis project. Bull. Am. Meteorol. Soc. 77, 437–472.
Kendall, M.G., 1975. Rank Correlation Methods, fourth ed. Charles Griffin, London, London, UK.
Kern, Z., Demény, A., Perşoiu, A., Hatvani, I.G., 2019. Speleothem records from the eastern part of Europe and Turkey—discussion on stable oxygen and carbon isotopes. Quaternary 2. https://doi.org/10.3390/quat2030031.
Kern, Z., Hatvani, I.G., Czuppon, G., Fórizs, I., Erdélyi, D., Kanduč, T., Palcsu, L., Vreča, P., 2020. Isotopic "altitude" and "continental" effects in modern precipitation across the Adriatic-Pannonian region. Water (Switzerland) 12. https://doi.org/10.3390/w12061797.
Klaus, J., Chun, K.P., Stumpp, C., 2015. Temporal trends in δ^{18}O composition of precipitation in Germany: insights from time series modelling and trend analysis. Hydrol. Process. 29, 2668–2680. https://doi.org/10.1002/hyp.10395.
Konecky, B.L., McKay, N.P., Falster, G.M., Stevenson, S.L., Fischer, M.J., Atwood, A.R., Thompson, D.M., Jones, M.D., Tyler, J.J., DeLong, K.L., Martrat, B., Thomas, E.K., Conroy, J.L., Dee, S.G., Jonkers, L., Churakova (Sidorova), O.V., Kern, Z., Opel, T., Porter, T.J., Sayani, H.R., Skrzypek, G., Abram, N.J., Braun, K., Carré, M., Cartapanis, O., Comas-Bru, L., Curran, M.A., Dassié, E.P., Deininger, M., Divine, D. V., Incarbona, A., Kaufman, D.S., Kaushal, N., Klaebe, R.M., Kolus, H.R., Leduc, G., Managave, S.R., Mortyn, P.G., Moy, A.D., Orsi, A.J., Partin, J.W., Roop, H.A., Sicre, M.A., von Gunten, L., Yoshimura, K., 2023. Globally coherent water cycle response to temperature change during the past two millennia. Nat. Geosci. 16, 997–1004. https://doi.org/10.1038/s41561-023-01291-3.
Kottek, M., Grieser, J., Beck, C., Rudolf, B., Rubel, F., 2006. World Map of the Köppen-Geiger climate classification updated. Meteorol. Zeitschrift 15, 259–263. https://doi.org/10.1127/0941-2948/2006/0130.
Krajcar Bronić, I., Barešić, J., Borković, D., Sironić, A., Mikelić, I.L., Vreča, P., 2020a. Long-term isotope records of precipitation in Zagreb, Croatia. Water (Switzerland) 12. https://doi.org/10.3390/w12010226.
Krajcar Bronić, I., Barešić, J., Sironić, A., Mikelić, I.L., Borković, D., Horvatinčić, N., Kovač, Z., 2020b. Isotope composition of precipitation, groundwater, and surface and Lake waters from the Plitvice Lakes, Croatia. Water (Switzerland) 12, 1–26. https://doi.org/10.3390/W12092414.
Krajcar Bronić, I., Horvatinčić, N., Obelić, B., 1998. Two decades of environmental isotope records in Croatia: reconstruction of the past and prediction of future levels. Radiocarbon 40, 399–416. https://doi.org/10.1017/s0033822200018282.
Krklec, K., Domínguez-Villar, D., Lojen, S., 2018. The impact of moisture sources on the oxygen isotope composition of precipitation at a continental site in central Europe. J. Hydrol. 561, 810–821. https://doi.org/10.1016/j.jhydrol.2018.04.045.
Kutiel, H., Maheras, P., 1998. Variations in the temperature regime across the Mediterranean during the last century and their relationship with circulation indices. Theor. Appl. Climatol. 61, 39–53. https://doi.org/10.1007/s007040050050.
Lancaster, S.T., Irrgeher, J., Dallmayr, R., Conrad, E., Hörhold, M., Bohleber, P., Behrens, M., Camin, F., Žagar, K., Vreča, P., Prohaska, T., 2025. $\delta(^{18}O/^{16}O)$ Determinations in Wader Using Inductivwly Coupled ilasma–Tandec Mass Splasma–ttry. Amal. shem. https://doi.org/10.1021/acs.analchem.5c02607.
Liu, Z., Bowen, G.J., Welker, J.M., 2010. Atmospheric circulation is reflected in precipitation isotope gradients over the conterminous United States. J. Geophys. Res. Atmos. 115, 1–14. https://doi.org/10.1029/2010JD014175.
López-Moreno, J.I., Vicente-Serrano, S.M., 2008. Positive and negative phases of the wintertime North Atlantic Oscillation and drought occurrence over Europe: a multitemporal-scale approach. J. Clim. 21, 1220–1243. https://doi.org/10.1175/2007JCLI1739.1.
Luukko, P.J.J., Helske, J., Räsänen, E., 2016. Introducing libeemd: a program package for performing the ensemble empirical mode decomposition. Comput. Stat. 31, 545–557. https://doi.org/10.1007/s00180-015-0603-9.
Lykoudis, S.P., Argiriou, A.A., 2011. Temporal trends in the stable isotope composition of precipitation: a comparison between the eastern mediterranean and central Europe. Theor. Appl. Climatol. 105, 199–207. https://doi.org/10.1007/s00704-010-0384-6.
Mann, H.B., 1945. Nonparametric tests against trend. Econometrica 13, 245–259.
Masiol, M., Zannoni, D., Stenni, B., Dreossi, G., Zini, L., Calligaris, C., Karlicek, D., Michelini, M., Flora, O., Cucchi, F., Treu, F., 2021. Spatial distribution and interannual trends of δ^{18}O, δ^2H, and deuterium excess in precipitation across North-Eastern Italy. J. Hydrol. 598, 125749. https://doi.org/10.1016/j.jhydrol.2020.125749.
Natali, S., Doveri, M., Franceschi, L., Giannecchini, R., Luppichini, M., Menichini, M., Zanchetta, G., 2023. Moisture sources and climatic effects controlling precipitation stable isotope composition in a western Mediterranean island (Pianosa, Italy). Atmos. Res. 294, 106987. https://doi.org/10.1016/j.atmosres.2023.106987.
Natali, S., Raco, B., Baneschi, I., Catania, M., Giorgi, C., Zanchetta, G., 2025. Unveiling climate signals and long-term variability from 30 years of precipitation isotopes in Pisa (Italy). In: EMS Annual Meeting Abstracts. https://doi.org/10.5194/ems2025-381. Ljubljana. Slovenia.
Nguyen, L.S.P., Nguyen, K.T., Griffith, S.M., Sheu, G.R., Yen, M.C., Chang, S.C., Lin, N.H., 2022. Multiscale temporal variations of atmospheric Mercury distinguished by the Hilbert–Huang transform analysis reveals multiple El niño–southern oscillation links. Environ. Sci. Technol. 56, 1423–1432. https://doi.org/10.1021/acs.est.1c03819.
Ogrin, D., 2015. Long-term air temperature changes in Ljubljana (Slovenia) in comparison to Trieste (Italy) and Zagreb (Croatia). Morav. Geogr. Reports 23, 17–26. https://doi.org/10.1515/mgr-2015-0014.
Palutikof, J.P., Conte, M., Casimiro Mendes, J., Goodess, C.M., Espirito Santo, F., 1996. Climate and climatic change. Mediterr. Desertif. L. 43, 86.
Papadimitriou, L.V., Koutroulis, A.G., Grillakis, M.G., Tsanis, I.K., 2016. High-end climate change impact on European runoff and low flows - exploring the effects of forcing biases. Hydrol. Earth Syst. Sci. 20, 1785–1808. https://doi.org/10.5194/hess-20-1785-2016.
Pebesma, E., 2018. Simple features for R: standardized support for spatial vector data. R J 10, 439–446. https://doi.org/10.32614/rj-2018-009.
Pezdič, J., 2003. Isotope fractionation of long term precipitation averages in Ljubljana (Slovenia). RMZ Mater. Geoenviron 50, 641–650.
Pezdič, J., 1999. Izotopi in geokemijski procesi. Naravoslovnotehniska Fakulteta. Oddelek za geologijo, Ljubljana.
Puntsag, T., Mitchell, M.J., Campbell, J.L., Klein, E.S., Likens, G.E., Welker, J.M., 2016. Arctic Vortex changes alter the sources and isotopic values of precipitation in northeastern US. Sci. Rep. 6, 1–9. https://doi.org/10.1038/srep22647.
R Core Team, 2021. R: a Language and Environment for Statistical Computing.
Rozanski, K., Araguás-Araguás, L., Gonfiantini, R., 1993. Isotopic patterns in modern global precipitation. In: Climate Change in Continental Isotopic Records. American Geophysical Union (AGU), pp. 1–36. https://doi.org/10.1029/GM078p0001.
Salamalikis, V., Argiriou, A.A., Dotsika, E., 2016a. Periodicity analysis of δ^{18}O in precipitation over Central Europe: time-frequency considerations of the isotopic "temperature" effect. J. Hydrol. 534, 150–163. https://doi.org/10.1016/j.jhydrol.2015.12.059.
Salamalikis, V., Argiriou, A.A., Dotsika, E., 2016b. Isotopic modeling of the sub-cloud evaporation effect in precipitation. Sci. Total Environ. 544, 1059–1072. https://doi.org/10.1016/j.scitotenv.2015.11.072.
Schirmer, M., Leschik, S., Musolff, A., 2013. Current research in urban hydrogeology - a review. Adv. Water Resour. 51, 280–291. https://doi.org/10.1016/j.advwatres.2012.06.015.
Schürch, M., Kozel, R., Schotterer, U., Tripet, J.P., 2003. Observation of isotopes in the water cycle - the Swiss National Network (NISOT). Environ. Geol. 45, 1–11. https://doi.org/10.1007/s00254-003-0843-9.
Sen, P.K., 1968. Estimates of the regression coefficient based on Kendall's tau. J. Am. Stat. Assoc. 63, 1379–1389. https://doi.org/10.1080/01621459.1968.10480934.
Sjostrom, D.J., Welker, J.M., 2009. The influence of air mass source on the seasonal isotopic composition of precipitation, eastern USA. J. Geochemical Explor. 102, 103–112. https://doi.org/10.1016/j.gexplo.2009.03.001.
Slovenian Environmental Agency (ARSO), 2025. ARSO METEO.
Sodemann, H., Schwierz, C., Wernli, H., 2008. Interannual variability of Greenland winter precipitation sources: lagrangian moisture diagnostic and North Atlantic Oscillation influence. J. Geophys. Res. Atmos. 113, 1–17. https://doi.org/10.1029/2007JD008503.
Stein, A.F., Draxler, R.R., Rolph, G.D., Stunder, B.J.B., Cohen, M.D., Ngan, F., 2015. NOAA's HYSPLIT atmospheric transport and dispersion modeling system. Bull. Am. Meteorol. Soc. 96, 2059–2077. https://doi.org/10.1175/BAMS-D-14-00110.1.
Stohl, A., Forster, C., Frank, A., Seibert, P., Wotawa, G., 2005. Technical note: the Lagrangian particle dispersion model FLEXPART version 6.2. Atmos. Chem. Phys. 5, 2461–2474. https://doi.org/10.5194/acp-5-2461-2005.
Stumpp, C., Klaus, J., Stichler, W., 2014. Analysis of long-term stable isotopic composition in German precipitation. J. Hydrol. 517, 351–361. https://doi.org/10.1016/j.jhydrol.2014.05.034.
Terzer-Wassmuth, S., Wassenaar, L.I., Welker, J.M., Araguás-Araguás, L.J., 2021. Improved high-resolution global and regionalized isoscapes of δ^{18}O, δ^2H and d-excess in precipitation. Hydrol. Process. 35. https://doi.org/10.1002/hyp.14254.
Trigo, R.M., Osborn, T.J., Corte-Real, J.M., 2002. The North Atlantic Oscillation influence on Europe: climate impacts and associated physical mechanisms. Clim. Res. 20, 9–17. https://doi.org/10.3354/cr020009.
Vachon, R.W., Welker, J.M., White, J.W.C., Vaughn, B.H., 2010. Monthly precipitation isoscapes (δ^{18}O) of the United States: connections with surface temperatures, moisture source conditions, and air mass trajectories. J. Geophys. Res. Atmos. 115, 1–17. https://doi.org/10.1029/2010JD014105.

Van Boxtel, G.J.M., et al., 2021. Gsignal: Signal Processing.

Vaughan, D., 2024. Slider: Sliding Window Functions.

Vreča, P., Bronić, I.K., Horvatinčić, N., Barešić, J., 2006. Isotopic characteristics of precipitation in Slovenia and Croatia: comparison of continental and maritime stations. J. Hydrol. 330, 457–469. https://doi.org/10.1016/j.jhydrol.2006.04.005.

Vreča, P., Krajcar Bronić, I., Leis, A., 2015. Isotopic composition of precipitation at the Station Portorož, Slovenia - period 2007-2010. Geologija 58, 233–246. https://doi.org/10.5474/geologija.2015.019.

Vreča, P., Krajcar Bronić, I., Leis, A., 2011. Isotopic composition of precipitation in Portorož (Slovenia). Geologija 54, 129–137. https://doi.org/10.5474/geologija.2011.010.

Vreča, P., Krajcar Bronić, I., Leis, A., Brenčič, M., 2008. Isotopic composition of precipitation in Ljubljana (Slovenia). Geologija 51, 169–180. https://doi.org/10.5474/geologija.2008.018Isotopic.

Vreča, P., Krajcar Bronić, I., Leis, A., Demšar, M., 2014. Isotopic composition of precipitation at the station Ljubljana (Reaktor), Slovenia - period 2007-2010. Geologija 57, 217–230. https://doi.org/10.5474/geologija.2014.019.

Vreča, P., Malenšek, N., 2016. Slovenian Network of Isotopes in Precipitation (SLONIP) - a review of activities in the period 1981-2015. Geologija 59, 67–84. https://doi.org/10.5474/geologija.2016.004.

Vreča, P., Pavšek, A., Kocman, D., 2022. SLONIP—A Slovenian web-based interactive research platform on water isotopes in precipitation. Water (Switzerland) 14. https://doi.org/10.3390/w14132127.

Vystavna, Y., Matiatos, I., Wassenaar, L.I., 2020. 60-year trends of δ^{18}O in global precipitation reveal large scale hydroclimatic variations. Glob. Planet. Change 195, 103335. https://doi.org/10.1016/j.gloplacha.2020.103335.

Wang, W., Chau, Chuan, Wing, K., Qiu, L., Chen, Y. bo, 2015. Improving forecasting accuracy of medium and long-term runoff using artificial neural network based on EEMD decomposition. Environ. Res. 139, 46–54. https://doi.org/10.1016/j.envres.2015.02.002.

Wassenaar, L.I., Terzer-Wassmuth, S., Douence, C., Araguas-Araguas, L., Aggarwal, P.K., Coplen, T.B., 2018. Seeking excellence: an evaluation of 235 international laboratories conducting water isotope analyses by isotope-ratio and laser-absorption spectrometry. Rapid Commun. Mass Spectrom. 32, 393–406. https://doi.org/10.1002/rcm.8052.

Welker, J.M., 2012. ENSO effects on δ^{18}O, δ^{2}H and d-excess values in precipitation across the U.S. using a high-density, long-term network (USNIP). Rapid Commun. Mass Spectrom. 26, 1893–1898. https://doi.org/10.1002/rcm.6298.

Welker, J.M., 2000. Isotopic (δ^{18}O) characteristics of weekly precipitation collected across the USA: an initial analysis with application to water source studies. Hydrol. Process. 14, 1449–1464. https://doi.org/10.1002/1099-1085(20000615)14:8<1449::AID-HYP993>3.0.CO;2-7.

Yang, H., Gao, Y., Zhao, F., Wang, J., 2024. An intelligent interval forecasting system based on fuzzy time series and error distribution characteristics for air quality index. Environ. Res. 251, 118577. https://doi.org/10.1016/j.envres.2024.118577.

Žagar, K., Ortega, L., Pavlič, U., Jamnik, B., Bračič Železnik, B., Vreča, P., 2024. Unravelling the sources contributing to the urban water supply: an isotope perspective from Ljubljana, Slovenia. J. Hydrol. 632. https://doi.org/10.1016/j.jhydrol.2024.130892.

Zhang, L., Wang, C., Hu, W., Wang, X., Wang, H., Sun, X., Ren, W., Feng, Y., 2024. Dynamic real-time forecasting technique for reclaimed water volumes in urban river environmental management. Environ. Res. 248, 118267. https://doi.org/10.1016/j.envres.2024.118267.